Theoretical Assessment on Shape-Dependent Optical Properties of Gold Nanostructures

Abdul Majid*, Alia Jabeen, Tanasam Shaheen,

Department of Physics, Hafiz Hayat Campus, University of Gujrat, Gujrat, Pakistan
*Corresponding author: ; aliajabeen777@gmail.com

Abstract

In the current work, detailed investigations on shape-dependent optical properties of gold nanostructures are carried out using the finite element method. The key objective of the work was to explore the optical response of differently shaped gold nanostructures. Five differently shaped gold nanostructures i.e. nanopyramid, nanocylinder, nanocone, nanosphere, and nanocube were considered to study the optical properties including skin depth, relative permittivity, refractive index, absorption cross-section, and extinction cross-section. The optical properties of gold appeared to depend on the shapes of nanostructures. The nanostructures with sharp apexes exhibit more skin depth in contrary to those having smooth surfaces. The surface Plasmon resonance (SPR) for the nanostructures was found maximum at 540 nm throughout the calculated range of wavelengths and the intensity of all the curves depends on the shape of the nanostructure.

Keywords—Optical properties, Surface Plasmon Resonance (SPR), Finite element method (FEM)

1 Introduction

The size and shape dependence of optical properties of metallic nanostructures is a striking research field due to their applications in devices and different areas of life [1-3]. The work on nanomaterials and related phenomena [4-6], which was initiated in the 9th century appeared as a research field in nanotechnology[7, 8] after the discovery of ruby gold nanoparticles. The current era is undoubtedly dominated by nanotechnology when research, development, applications, and industrial activities are concerned [9-11]. The realization of metallic nanoparticles with a focus on gold and silver nanoparticles due to their striking properties and variety of applications is an important research outcome. Gold nanoparticles (Au-NPs) have gained significant importance in recent decades owing to their noteworthy applications. The researchers have been trying hard to further explore the properties of Au-NPs, which is obvious from current activities across the globe and surveys of published literature. When Au-NPs are allowed to disperse in aqueous solutions, they are found to be more chemically stable as compared to silver nanoparticles [12, 13]. A number of ways have been used to fabricate distinctly shaped and sized nanoparticles [14]. They have applications in medical science in cancer treatment [15], bio-sensing [16], and drug delivery [17-19]. The usage of Au-NPs in electrochemical applications is also a growing field [20]. The analysis of elementary physical effects and exploring the relevant phenomenon occurring in Au-NPs has been a hot research topic recently [20].

The metallic nanoparticles, when exposed to light, exhibit novel behavior that can be studied via different techniques based on light-matter interaction. The nanomaterials whose optical properties indicate their activity in the visible region of the electromagnetic spectrum are attractive for devices and applications [21]. The optical phenomenon includes transmission, reflection, absorption, excitations, recombination kinetics, excitonic features, surface plasmonics, quantum confinement, etc., which open up the road to broad applications of metal nanoparticles [22, 23]. The optical properties basically include skin depth, refractive index, relative permittivity, absorption, and extinction cross-section, which are highly material-dependent. These exhibit significant variations when the size or shape of metal nanoparticles is altered. Like other

ISSN: 2523-0379 (Online), ISSN: 1605-8607 (Print)
DOI: https://doi.org/10.52584/QRJ.2102.09

metals, when the Au-NPs are exposed to light, the photons interact with conduction electrons to undergo absorption as well as scattering of light, as explained by Mie theory [24, 25].

It is well known that metallic nanoparticles exhibit plasmonic response when irradiated by electromagnetic waves. One of the prime reasons behind the exceptional research interest in Au-NPs is their optical response involving surface plasmons [26]. Basically, there are plenty of conduction electrons present in Au-NPs that interact with electromagnetic radiations in order to generate striking optical phenomena [27]. In response to incident electromagnetic waves, the collective oscillations of electrons that appeared in the metal-dielectric interface are termed localized surface plasmon resonance (LSPR), which strongly depends on the size, shape, and dielectric environment of the nanoparticles. The alterations made in the refractive index of the outer dielectric environment make surface plasmons more sensitive and provide the basis for surface plasmon resonance spectroscopy [13]. This property is affected by the size of the nanoparticles in such a way that the behavior is different for large and small nanoparticles. For small nanoparticles having a size up to 50 nm, the dipolar response can be used to differentiate intrinsic as well as extrinsic effects. On the other hand for larger nanoparticles the phenomena of absorption and scattering of light are dominated [13]. The absorption (scattering) spectra give information about the number of photons absorbed (scattered) by nanoparticles that help to explore the properties of the material. The sum of absorption and scattering cross-section is referred to as extinction cross-section that provides information on overall interaction and observation of resonance peak at a particular frequency. Besides the size-dependent effects, the optical properties are greatly affected by the shapes of nanoparticles [28]. By changing the outer dielectric environment, nanoparticles having sharp apexes are reported to be more sensitive to optical phenomena [13]. The maximum optical response has been observed for nano-branches and the minimum for nano-spheres in comparison to nano-cubes, nano-rods, and nano-bipyramids. The shape-dependent optical properties of surface plasmons are highly desired as they have the potential to offer widespread applications [29].

In recent years, substantial research has been carried out in order to study the shape-dependent attributes of Au-NPs because of their promising application in several scientific as well as technological applications [30-33]. The prior investigations have revealed the peculiar chemical as well as physical properties of Au-NPs are greatly affected by their morphology having distinct shapes like plates, spheres, cubes, and rods. These morphologies showed different optical, electronic, and catalytic properties. Such shape-dependent characteristics have been ascribed to the changes within the NP-surface plasmon resonance, crystal surfaces as well as surface energies, etc.

Despite the availability of rich literature on the optical properties of Au-NPs, much less is known about their shape dependence. Owing to the development of material synthesis and crystal growth technologies in the recent past, the realization of nano-materials of different shapes has become possible. This work is carried out with the motivation to provide initial predictions on shape-dependent optical properties of Au NPs for use in future miniature devices and applications. The five distinctly shaped gold nanostructures including Nanopyramid, Nanosphere, Nanocone, Nanocylinder, and Nanocube were designed, each having a maximum size of 100 nm. The aspect ratio varied from shape to shape as some of the nanostructures have smooth surfaces and the others have sharp apexes. The finite element method, implemented in the simulation package COMSOL Multiphysics was employed to design the structures of Rekic gold and study the optical properties.

2 Methodology

In the current work, the optical properties of gold nanostructures in the visible region of the electromagnetic spectrum were studied by using the simulation package COMSOL Multiphysics (version 5.1a). The method adopted to model geometry and extraction of results for the problem to be investigated is termed as Finite Element Method (FEM) which makes the basis for obtaining results [29, 34]. This FEM basically consists of three main steps [35]; namely pre-processing, solver, and post-processing relevant to geometry and mesh design, solving mathematical equations in the model, and obtaining suitable results respectively. Nanostructures with a size of about 100 nm were modeled with different shapes as nanopyramid, nanocone, nanocube, nanocylinder, and nanosphere, and then all of them were subjected to visible light separately. The material of nanostructures was taken as gold (Rakic) and an RF module was used to simulate the structures. The dielectric environment was such that the nanostructures were placed in the air. The entire shapes were studied under identical boundary conditions and under the same dielectric environment. A Perfectly Matched Layer (PML) was used to solve the problem with scattering boundary conditions. The structures were irradiated by visible electromagnetic radiations in the spectral region of 400 nm to 700 nm. The optical properties including skin depth, refractive index, relative permittivity, absorption, and extinction cross-section were investigated in detail.

3 Results and Discussions

The interaction of electromagnetic waves with gold nanostructures was comprehensively studied in this work to calculate the optical properties and investigate the shape dependence. The computed results are described below.

3.1 Skin depth

When a material is exposed to electromagnetic waves, an interaction between them takes place in such a way that some portion of waves is reflected from the surface and another portion tends to propagate in the material to a certain depth. The distance to which the electric field's amplitude in the material becomes 1/e of its value at the surface is referred to as skin depth [36]. The relation of frequency f and skin depth is $\delta = \sqrt{\frac{\rho}{\pi f \mu_r \mu_o}}$ where δ, ρ, and f are skin depth, resistivity, and frequency of incident light respectively. The skin depth of a conductor is inversely proportional to the frequency of incident radiation and related directly to the resistivity. The skin depth calculated for the Au nanostructures as a function of incident wavelength is shown in Fig. 1. The results indicate that skin depth varies not only with wavelength but also with the shape of nanostructures. The value of skin depth increases from 400 to 490 nm and decreases beyond it throughout to 700 nm. The skin depth for all structures peaks at 490 nm whereas the values of height and Full width half maximum (FWHM) of the peak are different for all structures. It appeared that the broadening and intensity of the peak is maximum for nano-pyramid whereas the same are minimum for nano-cylinder. The comparison of values of skin depth reveals that its values are found in decreasing order of nano-pyramid, nano-cube, nano-sphere, nano-cone, and nano-cylinder respectively. The value of FWHM calculated for the five nano-structures came out as 1.77 nm, 1.75 nm, 1.76 nm, 1.76 nm, and 2.47 nm for nano-cone, nano-cube, nano-cylinder, nano-pyramid and nano-sphere respectively.

In the region 400- 490 nm, the variation is consistent with relation (1) but the situation is different beyond 490 nm as the classical trend of skin depth is not followed. The maximum value of skin depth calculated for all the shapes is smaller than the size of the nano-structures (i.e.; 100 nm); therefore, the scattering of light from the surface contributes to the resistivity of the material [37]. The decrease in skin depth and hence the resistivity beyond 490 nm will cause an increase in skin conductivity and hence the surface current density.

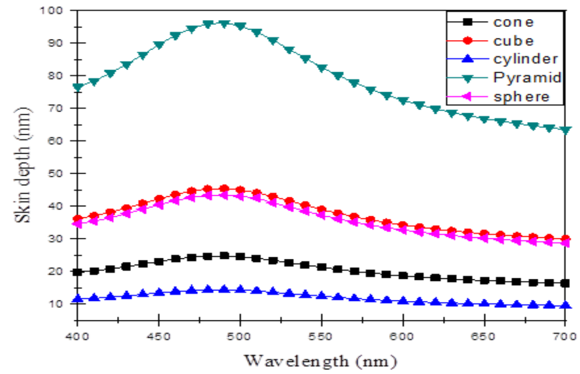

Fig. 1: Skin Depth of Gold Nanostructures; nano-cone, nano-cube, nano-cylinder, nano-pyramid, nano-sphere as a function of wavelength.

Now, let us compare the skin depth of bulk gold and the nanostructures. For two of the five nanostructures, the skin depth exceeds the bulk gold skin depth (approximately 38.46 nm for Rakic gold- obtained from COMSOL). This is because the properties of materials become more vibrant at the nano-scale. The metals with appreciable conductivity work in visible as well as near-infrared regions, most of the current flows on the surface and in a very small region of total volume. It is reported that the amount of electric current, which flows in a very small portion of the total volume, is confined below the air-medium interface of less than ten nanometers in agreement with the literature [38]. Thus, the peak is observed in the skin depth of gold for various shapes. In the case of our material, skin depth is maximum at 490 nm and is lowest at 700 nm.

It can be seen in Fig. 1 that for the wavelength range 400 nm $\leq \lambda \leq 700$ nm, skin depth increases with an increase in wavelength. An increase to about 490 nm indicates that the blue and green wavelengths of the electromagnetic spectrum are absorbed significantly by conductors, hence more skin depth due to current. The skin depth reduces after 490 nm until 700 nm which shows that the free electrons in the conductor reemit the red wavelengths of the electromagnetic spectrum.

The skin depth appeared to change with the shape of the nanostructures. Since the volume of the structures is the same, the changes in skin depth are obviously due to the difference in geometry[39]. Some of the structures have sharp edges thus the flow of skin current caused by incident electromagnetic waves varies from one shape to another. As the shape changes, the flow of electrons (that are contributing to skin current) as well as their collisions among themselves and with the skin of the conductor also varies. The plots showed that skin depth is maximum for nano-pyramid and minimum for nano-cylinder which is due to the reason that the apexes of nano-pyramid are sharp while smooth for the cylinder. The sharp edges tend to diffract the light that gets penetrated in the conductor more readily than a cylinder. The smooth surface of nano-cylinder with round edges doesn't penetrate the waves very much, hence, fewer collisions among electrons are likely. Though the nano-cube has edges that are not sharper than that of a nano-pyramid, the top surface as well as side walls of the cube are smooth, only the corners are sharp. Hence, diffraction in this case is more than those of nano-cylinder, nano-sphere, and nano-cone but less than that of nano-pyramid due to which the current in conductor flows sharply due to its sharp edges. If the corners of the cube are removed, then it becomes a sphere and hence both are smooth manifolds due to which they should show a minor difference in skin depth. Nano-cone has a little bit much sharper apex than the cylinder, hence the skin current for the nano-cone is less than that of the nano-sphere.

Besides the above-described effects, an important aspect may be the surface roughness within the bulk counterparts. Surface roughness could induce changes within the potent surface area along with the alteration in the electromagnetic interactions referring to the variation in the skin depth. This impact is specifically important when a comparison of skin depth of nanostructured materials with their relevant bulk counterparts is made. In addition to this, the surface roughness over the bulk materials could introduce specific features at the nanoscale. These features could be due to a number of reasons like grain boundaries, crystalline defects, or any other surface defects. As the EM waves interact with the rough surfaces the diffraction phenomenon along with the multiple scattering phenomenon occur, that impressively modify the apparent skin depth of the materials.

Thus, the variation in the plots of skin depth is just because of variation in shapes. The more the sharp edges of an object, the more skin depth because of the motion of electrons and collisions in the edge regions.

3.2 Refractive Index

Refractive index is such a property of optical media which is the ratio of the speed of light in a vacuum to the speed of light in the medium [40], [32]. It is the measure of variation in the speed of light as it changes its path from vacuum to any other medium. The refractive index of the majority of the materials is complex, consisting of two parts; real and imaginary part. Thus, the complete refractive index is given by $\tilde{n}=n+ik$, where n and k indicate the real and imaginary parts respectively. The real part provides information about the ratio of the speed of light in a vacuum to a medium while the imaginary part tells about absorption of incident light by the material. For the majority of materials, like metals, the value of k is equal to or greater than 1. In such cases, the absorption of incident electromagnetic waves by the material is very strong such that the wave is unable to penetrate for longer wavelengths.

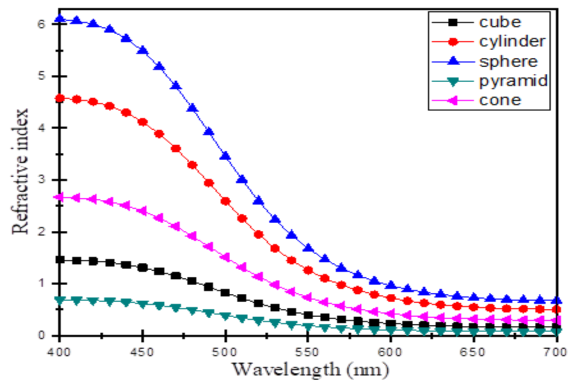

Fig. 2: Refractive Index of Gold Nanostructures; nanocone, nanocube, nanocylinder, nanopyramid, nanosphere, as a function of wavelength.

Under the irradiation of electromagnetic waves, all of the gold nanostructures tolerated a change in their refractive index that varied from one shape to another. The variations in the refractive index of gold (real part) nanostructures are plotted as a function of wavelength as shown in Fig. 2. The results show that the property varies not only with the wavelength of incident radiation but also with the shapes of nanostructures. The refractive index for all studied nanostructures decreases with an increase in wavelength and a sharper decrease is observed after 450 nm throughout the calculated range of wavelengths. The behavior for all the structures is the same in regions 650 nm to 700 nm where no further decrease in the refractive index takes place[41, 42]. It appears that the refractive index is maximum for the nanosphere and minimum for the nano-pyramid[43]. The comparison of the refractive index for all nanostructures exposes that its values are found in ascending order for nano-pyramid, nano-cube, nano-cone, nano-cylinder, and nano-sphere.

The variations in the patterns of refractive indices for all nanostructures reveal that it decreases by increasing the wavelength of light from 400 nm to 700 nm as described above. The refractive index has an inverse relation with the wavelength of light as frequency doesn't change from one medium to another. The inverse relation between refractive index and wavelength ($n\alpha\frac{1}{\lambda}$) is obvious from the plotted patterns which show a decrease of n for the entire calculated range of wavelengths.

The plots indicate that the refractive index patterns have very small penetration in the material. The incident photons can either reflect from the surface or refract as they interact with matter. In the case of metals, the refraction of photons owes to absorption by electrons and then their re-emission [44]. Regardless of wavelength, the majority of photons get absorbed by metal electrons as per energy levels and bands of the material. It is known that metals have complex indices of refraction for different ranges of wavelengths [45] because the metallic electrons respond to the incoming radiations either by absorption or by emission of photons. If the response of the electrons is not quick due to a number of reasons, a time lag between incoming and emitted radiations exists which leads to a complex index of refraction. The analysis of such complex optical properties may provide important information on the material. According to Lorentz and Drude models, there is no absorption of waves at high frequencies and metal behaves as transparent material. It is only due to the fact that at these frequencies, free electrons present in metals don't respond instantly to the incoming radiations [45]. Since gold is metal, the value of k approaches unity or higher which leads to the propagation of waves for small wavelengths and hence incident light does not penetrate further because of strong absorption. The absorption is hence maximum for longer wavelengths due to which we see a gradual decrease in wavelength beyond 550 nm.

The trend shown in Fig. 2 indicates that the refractive index of gold varies not only with wavelength of incident light but also with the shapes of the nanostructures. The nano-pyramid exhibited the least refractive index which points to a maximum speed of light in this structure. The speed of the incident electromagnetic wave inside the pyramid shows that the wave propagates more readily in it. The waves reflected from the sharp apexes of the pyramid support the incoming wave due to which they penetrate longer in the material. It is obvious from the plots of skin depth of nanostructures that it is maximum for nano-pyramids, thus skin depth and refractive index are interrelated in the case of pyramid. The waves with maximum speed can penetrate the conductor to some longer depth, thus the more the refractive index more the skin depth. The highest value of refractive index for nano-sphere shows that the propagation speed of incident electromagnetic waves inside the material is very slow due to which the waves cannot penetrate to more depth that points to the small skin depth. The refractive index for three other nanostructures increases for nano-cylinder, nanocone, and nanocube in the ascending order respectively. This is due to the fact that light can travel faster in a nanocube, due to its sharp edges, in comparison to nanocylinder and nanocones as they have comparatively smooth surfaces.

The nanopyramid structures seem to have the highest skin depth while having the least refractive index. This may be due to the existence of a hotspot within the nanoparticle environment that is predominant within the sharp-corned structures such as the nanopyramids in contrast with the spherical nanoparticles [30, 31]. This phenomenon has a substantial impact on the interaction of light with matter. Such hotspots are considered through the localized EM enhancements, which emerge at the sharp corners as well as edges of the nanoparticles, giving rise to amplified scattering, absorption as well as field confinement. Consequently, the production of the hotspots could provide enhanced interactions of the photons having the localized surface plasmon resonance (LSPR) of the nanoparticles. However, the impact of the hotspots is beyond the scope of this paper and hence not considered in this paper.

3.3 Relative permittivity

The permeability of a material basically describes the capability to get polarized under the application of an electric field [46]. It is also defined as the ability of a material to permit the transmission of an electric field [47]. Relative permittivity, on the other hand, is the ratio of the permittivity of medium to the permittivity of free space. It is sometimes called as dielectric constant of the material. For metals, the dielectric constant may be complex showing real and imaginary parts and the imaginary part deals with absorption loss just as the imaginary part of the refractive index provides information about the absorption of waves incident on the surface.

The variation in the relative permittivity of distinctly shaped nanostructures as a function of the wavelength of incident electromagnetic radiations is given in Fig.

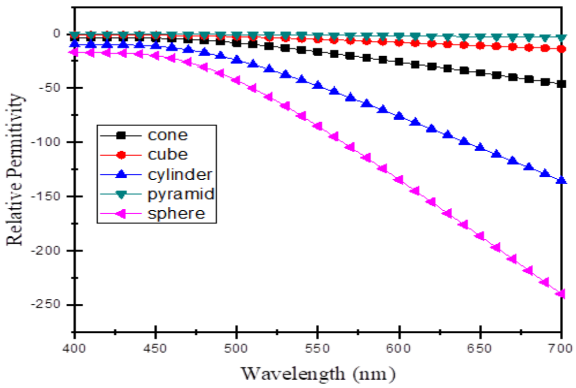

Fig. 3: Relative permittivity of Gold Nanostructures; nanocone, nanocube, nanocylinder, nanopyramid, and nanosphere, as a Function of Wavelength is simulated.

3. It appears that relative permittivity varies not only with the wavelength of incident radiation but also with the shapes of gold nanostructures. A rapid decrease in the permittivity of the material is seen at about 465 nm and decreases up to 700 nm. It can be seen that the property for all nanostructures decays slowly from 400 nm to 460 nm, and then a rapid decrease appears. Moreover, the plots for all nanostructures have negative permittivity values ranging from 0 to -250. Besides these, the permittivity of gold nanostructures is maximum for nanopyramid and holds a descending order from nanopyramid to nanocube, nanocone, nanocylinder, and nanosphere, overall calculated range of wavelengths.

In the case of metals, the real part of permittivity remains negative because the frequency of incident radiation is smaller than plasma frequency and free electrons contribute to the property [48]. It is this negative valued permittivity that results in the imaginary part of the refractive index [49]. The permittivity of gold is plotted in accordance with the Drude model. It appears in Fig. 3 that the relative permittivity of gold nanoparticles decreases with an increase in wavelength. The relation between relative permittivity and wavelength can be derived by a simple method. Since we know that $\lambda = \frac{c}{f}$ that points to an inverse relation between wavelength and relative permittivity. Hence it is the only reason behind the decay curve of permittivity over a calculated range of wavelengths. From the plots it is clear that the ability of gold (rakic) to transmit the no of lines of electric field, i.e. relative permittivity, in the blue region of the optical spectrum, decreases slowly but as we move to green and red, a rapid decay is observed. Hence, for a material to allow transmission on more electric-field lines, it must be operated with the blue region of the visible spectrum. The propagation of electromagnetic waves in matter is studied via the relation between the refractive index and the relative permittivity of the material. For most of the materials, μ is very close to μ_0 thus $n \cong \sqrt{\epsilon_r}$. Our results of relative permittivity and refractive index agree with this relation and both of the properties tend to decrease with an increase in wavelength.

From the plots, it appears that the relative permittivity varies from one shape of nanostructure to the other over the visible region from 400 nm to 700 nm. It means that by changing the shape/structure of gold nanoparticles, this optical property changes. Therefore, we can say that ϵ_r of gold nanoparticles also depends on geometry. From Figure 3, it can be seen that relative permittivity is minimum for the nanosphere and maximum for the nano-pyramid. It means that the nano-pyramid has more ability to permit the E-field lines to pass than the nano-sphere. We can relate it with the refractive index of a nano-pyramid as it is minimum for this shape, meaning that the speed of light in the nanoparticle is maximum thus refractive index is minimum. The more no. of lines inside the pyramid power each other with collisions, hence more speed, thus nanopyramid has the smallest refractive index and maximum relative permittivity. On the other hand, the nano-sphere has the smallest relative permittivity among all nanostructures, which shows that it doesn't have much ability to allow more electric field lines to pass. The reason is that a sphere has a smooth round surface and a pyramid has sharp edges, when light falls on them, a nano-sphere due to its round shaped boundary doesn't allow more lines to pass while a pyramid due to sharp apexes has more probability to pass them, because the reflected waves power more waves to pass through them. Similarly, the refractive index is maximum for the nano-sphere which shows that the speed of light is minimum, as there are fewer waves inside the sphere so the speed is minimum as there will be no collision among waves inside it. Moreover, the relative permittivity of nano-cylinder, nano-cone, and nano-cube is in between. Both the optical properties; refractive index and relative permittivity are related in this case. If one property is maximum for a nanostructure, the other is minimum for it as it can be seen from both patterns. Relative permittivity is in ascending order from nano-cylinder to nano-cone and nano-cube, and refractive index is in descending order from nano-cylinder to nano-cone and nano-cube. Thus, more no of lines inside the nanostructure lead to the minimum refractive index.

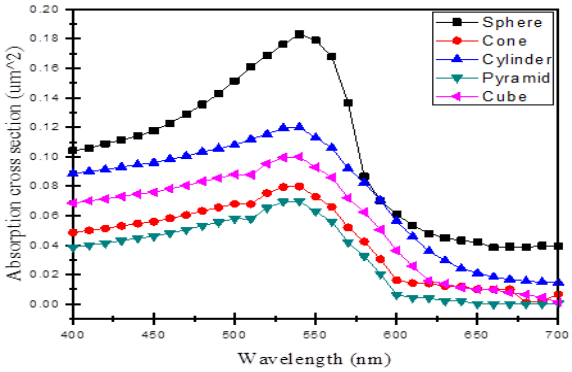

Fig. 4: Absorption Cross Section of Gold Nanostructures; nanocone, nanocube, nanocylinder, nanopyramid, nanosphere, as a Function of Wavelength.

3.4 Absorption Cross Section

Nanoparticles of noble metals exhibit Surface Plasmon Resonance (SPR) at optical frequencies that enable them to absorb and scatter visible light, efficiently [50]. Absorption cross-section is basically a particular cross-section of an object to absorb incident electromagnetic waves and also corresponds to the amount of incident light that has been absorbed by the object. Absorption is shape and size-dependent as it has also been determined by several studies. Under the irradiation of electromagnetic waves, the following results (Fig. 4) have been obtained from the calculations.

The variation in the absorption cross-section of different nanostructures as a function of wavelength is given in Fig. 4. The results plotted here reveal that the absorption cross-section not only varies with wavelength but also with the shape of nanostructures. It appears that the absorption cross-section for all differently shaped nanostructures peaks at the wavelength 540 nm, over a calculated range of wavelengths; from 400 nm to 700 nm. The results also indicate that the broadening and intensity of the peak are maximum for the nanosphere and the values are minimum for the nanopyramid. The overall comparison of the absorbance of nanostructures directs that the values are found in decreasing order for nanosphere, nanocylinder, nano-cube, nano-cone, and nano-pyramid throughout the visible region, plotted here. The value of the absorption cross-section increases from 400 nm to 540 nm and decreases beyond it throughout to 700 nm.

The plots in Fig. 4 indicate that the absorbing efficiency; and absorption cross-section, of all gold nanostructures, vary from one structure to another thus we can say that the absorption cross-section is shape-dependent.

Basically, it also corresponds to that particular involved in absorption, as well as the ability of a particle to respond to a particular photon. It is obvious that the absorption spectra of all of the gold nanostructures have a broad resonance at about 540 nm caused by the collective oscillations of conduction electrons. It means that the free electrons present in gold respond to particular photons of energy, as a result, they begin to oscillate and hence surface plasmon resonance. For all nanostructures, the absorbance of photons is maximum when the wavelength is 540 nm. Thus, for gold (rakic) nanoparticles, the SPR is obtained at 540 nm. The shape of gold nanoparticles highly affects the absorption cross-section. The gold nano-spheres have maximum absorbance than all other nanostructures, which means that the nanosphere has more probability to absorb photons of incident light because of its smooth round shape. The minimum optical absorption is seen by the gold nano-pyramid as it has sharp edges from which other processes like reflection and scattering may also be possible. All the nanostructures with smooth surfaces are more likely to absorb photons by showing maximum absorption cross-section.

Nano-cylinder has more optical absorption of incident photons than other nanostructures except for nanosphere. It is because that cylinder has smooth top and bottom surfaces with round edges hence providing more probability of absorption. The other nanostructures have optical absorption in a decreasing order for nano-cube, nano-cone, and nano-pyramid respectively which is only due to the shape of particular nanostructure as described above. It is clear that the nanoparticles provide more cross-sectional area to absorb the incoming photons in increasing order for nano-pyramid, nano-cone, nano-cube, nano-cylinder, and nano-sphere respectively. Thus, the optical absorption dependence of gold nanostructures directs that if more absorption is required then the shape of the nanostructure must be modified to achieve the desired surface plasmon resonance (SPR).

3.5 Extinction Cross Section

Besides absorption of incident light, gold nanoparticles exhibit scattering spectra when interacting with light. The colors exhibited by metals are due to scattering properties. As mentioned above, the absorption spectrum of gold nanoparticles shows the photons of incident light that tend to resonate with the electrons' oscillations, however, scattering spectra provide information about photons that are scattered by the surface without making interaction with electrons' oscillations. Extinction is basically the sum of absorption

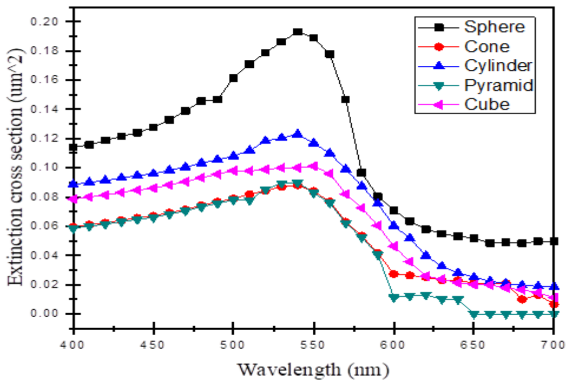

Fig. 5: Extinction Cross Section of Gold Nanostructures; nanocone, nanocube, nanocylinder, nanopyramid, nanosphere, as a Function of Wavelength

and scattering, and extinction cross section is the sum of absorption cross section and scattering cross section, describing the particle's efficiency of removal of photons from incident light and extinction spectra give information of SPR of gold nanostructures as well. The variation in the extinction cross-section of differently shaped nanostructures as a function wavelength of incident electromagnetic radiation is given in Fig. 5. The results indicate that the extinction of incident waves varies with wavelength as well as from one shape of nanostructure to another. Extinction cross section for all of the nanostructures peaks at 540 nm of incident wavelength and maximum for nano-sphere while minimum for nano-pyramid. The comparison of values of extinction cross-section reveals that its values are found in decreasing order for nano-sphere, nano-cylinder, nano-cube, nano-cone, and nano-pyramid, respectively throughout the calculated range of wavelengths (from 400 nm to 700 nm).

We know that extinction is basically the information of incident electromagnetic waves after their interaction with matter. It gives information about the particle's ability to remove photons from incident radiation by the processes of absorption and scattering [51]. The extinction cross-section is basically the sum of the absorption cross-section and scattering cross-section. Thus, it comes out to be more than absorption cross section because contribution from scattering is involved too. In our case, the scattering is very minimal and has its roots in Rayleigh scattering because the size of the particle is very minimal as compared to wavelength. It can be seen that the plasmonic wavelength for gold nanoparticles is the same as obtained from absorption cross-section spectra, meaning that all nanostructures have localized surface plasmon resonance at 540 nm.

The spectra for all of the nanostructures are shifted to maximum values as compared to absorption spectra due to the addition of scattering spectra. It indicates that nanoparticles scatter light too, which scatters in all directions as revealed by Rayleigh scattering. The extinction spectra for nano-cone and nano-pyramid are very close to each other as is not the case with absorption spectra. It is because of nanopyarmid which is shifted more than nanocone. It indicates that nanopyramid is more likely to scatter light than nanocone and hence overlaps with its spectra. Because of the sharp apexes and edges of the nanopyramid, it scatters more. The decreasing order of nanostructures for nanosphere, nano-cylinder, nano-cube, nano-cone, and nano-pyramid shows that the nanosphere is more likely to remove photons of particular wavelength and energy from incident electromagnetic radiation than other nanostructures. It has already been seen from absorption spectra that it is maximum for the nano-sphere and holds the decreasing order same as extinction spectra. Thus we can say that there is no dominant change in both plots, indicating that scattering is very minimal because extinction is the sum of absorption and scattering cross-sections. The comparison of all nanostructures reveals that extinction spectra are maximum for nanocylinder than all other nanostructures except nanosphere, hence, we can say that the scattering and absorption responses of nanocylinder are more than other structures indicating that the probability of removal of photons from radiation is second maximum for nanocylinder as it is highest for nanosphere. The optical scattering and absorption contributions are highly shape-dependent as per the findings of this work [52]. It is therefore recommended that, if more extinction of incident wave is desired for a particular nanoparticle, the modifications in shape should be made in addition to the variations in size.

4 Summary

In order to determine the optical properties of five different shapes of nanostructures, visible light was allowed to interact with differently shaped gold nanostructures using the finite element method. The computed results indicated that the optical properties of gold highly depend upon the shapes of nanostructures. The optical properties; skin depth, refractive index, relative permittivity, absorption cross-section, and extinction cross-section, are found to not only vary with wavelength but with the shape of nanostructures. The calculated skin depth and refractive index of gold are directly related to each other for all the shapes. Moreover, the refractive index is concluded to be inversely related to relative permittivity. The nanostructures with sharp apexes exhibit more skin depth, on the other hand, smooth-surface nanostructures offer more geometrical cross-section to absorb incident electromagnetic waves as well as exhibit low refractive index. The nanostructures expose plasmonic response when irradiated by electromagnetic waves and Surface Plasmon Resonance (SPR) for all of these nanostructures peaks at 540 nm. The intensity of all the curves depends on the shape of the nanostructure. From all of these indications of results, we can conclude that the optical properties of gold are shape-dependent. Furthermore, the results revealed the various shapes of Au-NPs may serve as potential candidates for several applications such as biosensing, plasmon-enhanced photovoltaics, optoelectronics, displays, etc.

References

[1] M. Mayer et al., ”Controlled living nanowire growth: precise control over the morphology and optical properties of AgAuAg bimetallic nanowires,” Nano Letters, vol. 15, no. 8, pp. 5427-5437, 2015.

[2] V. Giannini et al., ”Plasmonic nanoantennas: fundamentals and their use in controlling the radiative properties of nanoemitters,” Chemical Reviews, vol. 111, no. 6, pp. 3888-3912, 2011.

[3] K. Javid et al., ”Double-diffusion convective biomimetic flow of nanofluid in a complex divergent porous wavy medium under magnetic effects,” Journal of Biological Physics, vol. 47, no. 4, pp. 477-498, 2021.

[4] K. Ariga, T. Mori, and J. P. Hill, ”Mechanical control of nanomaterials and nanosystems,” Advanced Materials, vol. 24, no. 2, pp. 158-176, 2012.

[5] D. Yadav et al., ”Hybrid nanomaterial and instability analysis of convective flow in permeable media,” Applied Nanoscience, pp. 1-15, 2021.

[6] A. Riaz et al., ”Thermal analysis of peristaltic flow of nanosized particles within a curved channel with second-order partial slip and porous medium,” Journal of Thermal Analysis and Calorimetry, vol. 143, no. 3, pp. 1997-2009, 2021.

[7] D. Schaming and H. Remita, ”Nanotechnology: from the ancient time to nowadays,” Foundations of Chemistry, vol. 17, no. 3, pp. 187-205, 2015.

[8] V. Sharma, K. Park, and M. Srinivasarao, ”Colloidal dispersion of gold nanorods: Historical background, optical properties, seed-mediated synthesis, shape separation and self-assembly,” Materials Science and Engineering: R: Reports, vol. 65, nos. 1-3, pp. 1-38, 2009.

[9] T. M. Khan et al., ”Theoretical–Computational Study of Atmospheric DBD Plasma and Its Utility for Nanoscale Biocompatible Plasmonic Coating,” Molecules, vol. 26, no. 16, p. 5106, 2021.

[10] A. Bahadar and M. Zwawi, ”Development of SWCNTs-reinforced EPDM/SBR matrices for shock absorbing applications,” Materials Research Express, vol. 7, no. 2, p. 025310, 2020.

[11] S. U.-D. Khan, R. Khan, and S. Hussain, ”Suitability of thermal plasma for solid waste treatment and non-thermal plasma for nano-scale high-tech plasmonic materials: a concise review,” Applied Nanoscience, pp. 1-16, 2022.

[12] T. M. Khan et al., ”Silver nanoparticle films by flowing gas atmospheric pulsed laser deposition and application to surface-enhanced Raman spectroscopy,” International Journal of Energy Research, vol. 44, no. 14, pp. 11443-11452, 2020.

[13] H. Chen et al., ”Shape-and size-dependent refractive index sensitivity of gold nanoparticles,” Langmuir, vol. 24, no. 10, pp. 5233-5237, 2008.

[14] J. Pérez-Juste et al., ”Gold nanorods: synthesis, characterization and applications,” Coordination Chemistry Reviews, vol. 249, nos. 17-18, pp. 1870-1901, 2005.

[15] L. C. Kennedy et al., ”A new era for cancer treatment: gold-nanoparticle-mediated thermal therapies,” Small, vol. 7, no. 2, pp. 169-183, 2011.

[16] K. Saha et al., ”Gold nanoparticles in chemical and biological sensing,” Chemical Reviews, vol. 112, no. 5, pp. 2739-2779, 2012.

[17] S. Andleeb et al., ”In vitro bactericidal, antidiabetic, cytotoxic, anticoagulant, and hemolytic effect of green-synthesized silver nanoparticles using Allium sativum clove extract incubated at various temperatures,” Green Processing and Synthesis, vol. 9, no. 1, pp. 538-553, 2020.

[18] M. U. A. Khan et al., ”Smart and pH-sensitive rGO/Arabinoxylan/chitosan composite for wound dressing: In-vitro drug delivery, antibacterial activity, and biological activities,” International Journal of Biological Macromolecules, vol. 192, pp. 820-831, 2021.

[19] P. Ghosh et al., ”Gold nanoparticles in delivery applications,” Advanced Drug Delivery Reviews, vol. 60, no. 11, pp. 1307-1315, 2008.

[20] S. Guo and E. Wang, ”Synthesis and electrochemical applications of gold nanoparticles,” Analytica Chimica Acta, vol. 598, no. 2, pp. 181-192, 2007.

[21] K. Kumar, S. V. Kailas, and T. S. Srivatsan, ”Influence of tool geometry in friction stir welding,” Materials and Manufacturing Processes, vol. 23, no. 2, pp. 188-194, 2008.

[22] . U.-D. Khan et al., ”Theoretical relation between halo current-plasma energy displacement/deformation in EAST,” Journal of Theoretical and Applied Physics, vol. 12, no. 1, pp. 23-31, 2018.

[23] U. Kreibig and M. Vollmer, ”Optical properties of metal clusters,” Springer Science & Business Media, 2013.

[24] R. Weerasekera et al., ”Mie-Theory-Based Investigation of the Effect of Size Distribution on the Surface Plasmon Absorption of Silver Nanoparticles,” in 2022 Moratuwa Engineering Research Conference (MERCon), 2022.

[25] A. Ikram et al., ”Controllable fabrication and characterization of gold nanoparticles: enhanced therapeutic approaches in cancer,” Open Journal of Science and Technology, vol. 2, no. 1, pp. 26-28, 2019.

[26] V. Amendola et al., ”Surface plasmon resonance in gold nanoparticles: a review,” Journal of Physics: Condensed Matter, vol. 29, no. 20, p. 203002, 2017.

[27] L. A. Austin, B. Kang, and M. A. El-Sayed, ”Probing molecular cell event dynamics at the single-cell level with targeted plasmonic gold nanoparticles: A review,” Nano Today, vol. 10, no. 5, pp. 542-558, 2015.

[28] P. K. Jain et al., ”Calculated absorption and scattering properties of gold nanoparticles of different size, shape, and composition: applications in biological imaging and biomedicine,” The Journal of Physical Chemistry B, vol. 110, no. 14, pp. 7238-7248, 2006.

[29] H. Ditlbacher et al., ”Spectrally coded optical data storage by metal nanoparticles,” Optics Letters, vol. 25, no. 8, pp. 563-565, 2000.

[30] C. Wang et al., "Importance of hot spots in gold nanostructures on direct plasmon-enhanced electrochemistry," ACS Applied Nano Materials, vol. 1, no. 10, pp. 5805-5811, 2018.
[31] O. Pryshchepa, P. Pomastowski, and B. Buszewski, "Silver nanoparticles: Synthesis, investigation techniques, and properties," Advances in Colloid and Interface Science, vol. 284, p. 102246, 2020.
[32] A. Bigdeli et al., "Towards defining new nano-descriptors: extracting morphological features from transmission electron microscopy images," RSC Advances, vol. 4, no. 104, pp. 60135-60143, 2014.
[33] Q. Wang et al., "Photonic interaction between quantum dots and gold nanoparticles in discrete nanostructures through DNA directed self-assembly," Chemical Communications, vol. 46, no. 2, pp. 240-242, 2010.
[34] Z. OC, "The finite element method," McGraw-Hill, London, 1977.
[35] C. Multiphysics, "3.4," COMSOL AB, Stockholm, Sweden.
[36] R. L. Olmon et al., "Optical dielectric function of gold," Physical Review B, vol. 86, no. 23, p. 235147, 2012.
[37] R. Sarvari, "Impact of size effects and anomalous skin effect on metallic wires as GSI interconnects," Georgia Institute of Technology, 2009.
[38] F. Koohyar, "Refractive index and its applications," J. Thermodyn. Catal, vol. 4, no. 02, 2013.
[39] L. B. Scaffardi and J. O. Tocho, "Size dependence of refractive index of gold nanoparticles," Nanotechnology, vol. 17, no. 5, p. 1309, 2006.
[40] R. Naeye, "Through the Eyes of Hubble: The Birth, Life and Violent Death of Stars," CRC Press, 1997.
[41] Y. Z. Shi et al., "Determination of size and refractive index of single gold nanoparticles using an optofluidic chip," AIP Advances, vol. 7, no. 9, 2017.
[42] P. Tuersun et al., "Refractive index sensitivity analysis of gold nanoparticles," Optik, vol. 149, pp. 384-390, 2017.
[43] N. Piri, A. Shams-Nateri, and J. Mokhtari, "The relationship between refractive index and optical properties of absorbing nanoparticle," Color Research & Application, vol. 41, no. 5, pp. 477-483, 2016.
[44] T. Iwata and G. Komoda, "Measurements of complex refractive indices of metals at several wavelengths by frustrated total internal reflection due to surface plasmon resonance," Applied Optics, vol. 47, no. 13, pp. 2386-2391, 2008.
[45] M. Fox, "Optical properties of solids," American Association of Physics Teachers, 2002.
[46] Z. Ahmad, "Polymer dielectric materials," in Dielectric Material, IntechOpen, 2012.
[47] R. Taherian and A. Kausar, "Electrical Conductivity in polymer-based composites: experiments, modelling, and applications," William Andrew, 2018.
[48] P. Tassin et al., "A comparison of graphene, superconductors and metals as conductors for metamaterials and plasmonics," Nature Photonics, vol. 6, no. 4, pp. 259-264, 2012.
[49] V. Yannopapas and A. Moroz, "Negative refractive index metamaterials from inherently non-magnetic materials for deep infrared to terahertz frequency ranges," Journal of Physics: Condensed Matter, vol. 17, no. 25, p. 3717, 2005.
[50] T. Götz et al., "Characterization of large supported metal clusters by optical spectroscopy," Zeitschrift für Physik D Atoms, Molecules and Clusters, vol. 33, no. 2, pp. 133-141, 1995.
[51] M. A. García, "Surface plasmons in metallic nanoparticles: fundamentals and applications," Journal of Physics D: Applied Physics, vol. 44, no. 28, p. 283001, 2011.
[52] M. Goyal and M. Singh, "Size and shape dependence of optical properties of nanostructures," Applied Physics A, vol. 126, no. 3, pp. 1-8, 2020.